

The effects of spin fluctuations on the tunneling spectroscopy in High- T_c Superconductors

C. L. Wu¹, Chung-Yu Mou^{1,2}, Darwin Chang^{1,3}

¹*Department of Physics, National Tsing Hua University, Hsinchu 30043, Taiwan*

²*National Center for Theoretical Sciences, P.O.Box 2-131, Hsinchu, Taiwan*

³*Stanford Linear Accelerator Center, Stanford University, Stanford, CA 94309, USA*

Abstract

We investigate the effects of spin fluctuations on the tunneling spectra of the NS junction. In the high junction resistance limit, the dip/hump structure observed in ARPES data for the high T_c superconductors is reproduced in a RPA treatment of the t-t'-J model. It is shown that the dip/hump structure weakens as doping increases as reflected in the data. In the other limit, we predict that the zero bias Andreev peak can coexist with the dip/hump structure. Furthermore, the c-axis tunneling spectra is found to be very similar to a recent STM data once these fluctuations are included.

{PACS numbers: 74.20.-z, 74.50.+r, 74.80.FP, 74.20.Mn }

While a great details about the spectral function for high- T_c superconductors (HTS) have been revealed by the angle resolved photoemission spectroscopy (ARPES) [1], a complete description of the superconducting state requires knowledge of the anomalous Green's function. Conventionally the tunneling spectroscopy has been considered as one of the tools which can probe the anomalous Green's function. In particular, measuring the subgap conductance of a junction consisting of a normal metal and a superconductor (NS) is the most convenient configuration for such a purpose. To calculate the conductance in the NS configuration, Blonder, Tinkham, and Klapwijk[2](BTK) developed a formalism using Bogoliubov-de Gennes (BdG) mean-field equations. The BTK theory has been phenomenologically extended to investigate the tunneling phenomena in various NS junctions[3]. On the experimental side, even though the d-wave BCS mean field theory captures some features of the superconducting state, the recent high resolution data from both ARPES and STM gives a more delicate picture. A new feature is the appearance of so called peak/dip/hump structure, which is most clearly seen along the [100] direction in the superconducting state for ARPES [4, 5] and for STM [6]. It has been suggested[7] that it stems from the coupling of electrons to the π resonance observed in neutron scattering studies[8]. This idea has been further explored both qualitatively[9] and quantitatively[10], confirming its validity. In addition to the peak/dip/hump structure, there are also indications that the quasi-particle peak seems not to be resolution limited[11]. These features indicate the need for a tunneling theory that includes the effect of fluctuations.

¹Work supported by the Department of Energy, Contract DE-AC03-76SF00515

In this work, we investigate the effects of the spin fluctuations on the tunneling conductance spectra along the [100] and [001] (c-axis) directions[12]. By using the Keldysh formulation, we first demonstrate that in the high junction resistance limit, the dominant contribution comes from the spectral function and the peak/dip/hump structure exists in this limit. This structure results from collective spin fluctuations and weakens as the doping δ increases as reflected in some of the recent data, such as in Ref.[13]. Since spin excitations are gapped, they induce little qualitative change in the subgap region. Instead, their main effect is to redistribute the spectral weight and thus changes the relative strength among currents due to difference tunneling processes. Therefore, to investigate the other limit when the subgap is dominated by the Andreev reflection, we define the *optimum matching* as the condition when the zero bias Andreev conductance peak reaches maximum. This corresponds to the $Z = 0$ case in the BTK theory. Under this condition, we show that the Andreev peak can coexist with the dip/hump structure, which should be observable in the recent future. Base on our analysis, we will also give a possible explanation on a recently observed c-axis STM data [14], which shows an unexpected step like feature in the negative bias in addition to the peak/dip/hump structure.

We start by considering a junction consisting of a 2D normal metal on the left (L) hand side ($-\infty < x \leq 0$) and a 2D superconductor ($a \leq x < \infty$, a is the lattice constant) on the right (R) hand side, governed by the Hamiltonian H_L and H_R respectively. The tunneling Hamiltonian that connects the surface points at $x = 0$ and $x = a$ is given by $H_T = \sum_y t(|y_L - y_R|)(c_L^\dagger c_R + c_R^\dagger c_L)$, where the summation is over lattice points along the interface, chosen to be in the y direction. We consider the simplest case when the lattice points along the interfaces are equally spaced and match the bulk lattice of the metal and the superconductor. The superconductor is assumed to have a square lattice with one of the axis parallel to the x direction. The total grand Hamiltonian is then given by $K = H_L - \mu_L N_L + H_R - \mu_R N_R + H_T$, where μ_L and μ_R are the chemical potentials and their difference $\mu_L - \mu_R$ is fixed to be the voltage drop eV across the junction.

The tunneling current can be calculated perturbatively by using the Keldysh formalism[15]. This approach was previously applied successfully to study a number of tunneling problems[16, 17]. We shall follow Ref.[16] and neglect the vertex corrections of H_T . The perturbation series in H_T can be then summed exactly. The contribution to the differential conductance $G = dI/dV$ can be classified into four terms due to different tunneling processes[16]: G_1 is due to particle to particle tunneling; G_2 is due to particle to particle tunneling with pair creation/annihilation as the intermediate state; G_3 is due to particle to hole tunneling; and G_A is the Andreev conductance. Because H_T is a tight binding model, all the Green's functions have to be replaced by the surface Green's functions that connect different points on the junction. Thus there is an extra integration over k_y and associated with each surface Green's function, there is a $t(k_y)$ factor. The function $t(k_y)$ characterizes the spread of the electron wave function along y direction when hopping across the junction and can be generally expanded in a cos Fourier series. Note that the bare surface Green's function, without being renormalized by H_T , is a 2×2 matrix $\hat{g}_0(\omega, k_y)$ in Nambu's notation[16], and its relation to the bare bulk Green's function $\hat{G}_0(\omega, k_x, k_y)$ is given by $\hat{g}_0(\omega, k_y) = \frac{2}{\pi} \int_0^\pi dk_x \sin^2(k_x) \hat{G}_0(\omega, k_x, k_y)$, where the momentum k is in unit $1/a$.

The relations of conductance G_α to the Green's functions can be best demonstrated in the limit when the metal is approximated by its bandwidth t_L with a constant density of state, i.e., $g_L(\omega, k_y) = -i/t_L \times \mathbf{I}$, where \mathbf{I} is a unit matrix. This avoids complications due to the band structure from the metal side. In this case, when $t(k_y) = t$ is a constant, the only dimensionless parameter is $\lambda \equiv t^2/(t_L t_R)$, where t_R is the hopping scale of the superconducting side. The junction conductance is then of order $\lambda e^2/\hbar$. For small λ , $G_1(V)$ is $O(\lambda)$ and is simply proportional to the single particle density of state[18]. Similarly, $G_2(V)$ is of order $O(\lambda^2)$ and probes $\int dk_y [\text{Im}(g_{0R,12}^r)]^2$, $G_3(V)$ is of the order $O(\lambda^3)$ and probes $\int dk_y \rho_{R,22} |g_{0R,12}^r|^2$. Here 1

and 2 are indices for Nambu notations, Green's functions with the index r are retarded and ρ is the spectral function. Since G_3 is subdominant to $G_2(V)$, $G_2(V) + G_3(V)$ is negative. Finally, the Andreev conductance is $O(\lambda^2)$ and probes $\int dk_y [(g_{0R,12}^r)]^2$. Overall speaking, for small λ , the total conductance is dominated by G_1 , corresponding to the large Z limit of the BTK theory. In the other limit when G_A dominates in the sub-gap region, the situation is more subtle. For s-wave BCS superconductors, the analytic mapping from Z to λ was obtained in Ref [16]. The optimum matching ($Z = 0$) does not occur at large λ because the mapping is not monotonic. In general, such analytic mapping does not exist, we shall resort to numerics to find the optimum matching condition.

We first consider a simple d-wave BCS superconductor described by

$$H_R^m = \sum_{k\sigma} \epsilon_k c_{k\sigma}^+ c_{k\sigma} - \sum_k \Delta_k (c_{k\uparrow}^+ c_{-k\downarrow} + h.c.), \quad (1)$$

where the dispersion $\epsilon_k = -2t_R[\cos(k_x) + \cos(k_y)]$, and the gap $\Delta(k) = \Delta_R[\cos(k_x) - \cos(k_y)]$. The metal side has the same Hamiltonian with $\Delta_L = 0$. Under the optimum matching condition, one obtains a single peak (the Andreev peak) in the total conductance near $V = 0$ [17, 12]. The Andreev peak obtained here is a result of subtle balance between $G_1 + G_A$ and $G_2 + G_3$. In fact, the effect of $G_2 + G_3$ is to bring down the quasi-particle peaks in $G_1(V)$ so that a single peak is manifested. As we shall see, such simple realization of the Andreev peak does not always happen in real high-Tc systems due to spin fluctuations.

To include the spin fluctuations, we shall work with the 2D $t - t' - J$ model. In the slave-boson method, the physical electron operators $c_{i\sigma}$ are expressed by slave bosons b_i carrying the charge and fermions $f_{i\sigma}$ representing the spin; $c_{i\sigma} = b_i^+ f_{i\sigma}$. The mean-field d-wave SC state is characterized by the order parameters $\Delta_0 = \langle f_{i\uparrow} f_{j\downarrow} - f_{i\downarrow} f_{j\downarrow} \rangle$, $\chi_0 = \sum_{\sigma} \langle f_{i\sigma}^+ f_{j\sigma} \rangle$ and the condensate of bosons $b_i \rightarrow \langle b_i \rangle = \sqrt{\delta}$. Eq.(1) is then the Hamiltonian for the spinons, f_i , with dispersion $\epsilon_k = -2(\delta t_R + J' \chi_0)[\cos(k_x) + \cos(k_y)] - 4\delta t_R' \cos(k_x) \cos(k_y) - \mu_R$ and $\Delta_R = 2J' \Delta_0$, where $J' = 3J/8$. We shall adopt the following numerical values $t_R = 2J$, $t_R' = -0.45t_R$, and $J = 0.13\text{eV}$ [10, 19]. The mean-field parameters χ_0 , Δ_0 and the chemical potential μ_R for different doping δ are obtained from a self-consistent calculation[10]. Next we include the spin fluctuations by perturbing around the mean field Hamiltonian H_R^m , i.e., we write $K_R = H_R^m + H'$, and treat H' as a perturbation. In order to account for the π resonance[8] as well as many other effects of spin fluctuations, we calculate the spin susceptibility in a modified random-phase approximation (RPA) as defined in Ref.[10, 19]. The usual RPA sums over selected sets of graphs for the spin susceptibility χ as shown in Fig.1(a) and gives rise to $\chi(\mathbf{q}, \omega) = \chi_0(\mathbf{q}, \omega) / [1 + \alpha J(\mathbf{q}) \chi_0(\mathbf{q}, \omega)]$ with $\alpha = 1$. Here, $J(\mathbf{q}) = J(\cos q_x + \cos q_y)$, $\chi_0(\mathbf{q}, \omega)$ is the *unperturbed* spin susceptibility due to the spinon bubbles and the π resonance emerges as the pole of the denominator. In the current approach, α is not one and is considered as a phenomenological parameter whose value is chosen such that the AF instability occurs right at the experimental observed value $\delta = 0.02$. For the material parameters we adopt, α is 0.34[10].

The inelastic scattering of electrons off the spin fluctuations is taken into account by incorporating χ into the self energy of the spinons in the lowest-order approximation. In the SC state, there are two different self-energies Σ_s and Σ_w as shown in Fig.1(b) and (c). The Green's function for spinons is calculated by $G_f(\mathbf{k}, \omega) = [G_{f0}^{-1}(\mathbf{k}, \omega) + (\Delta_k + \Sigma_w)^2 G_{f0}^{-1}(-\mathbf{k}, -\omega)]^{-1}$ with $G_{f0}(\mathbf{k}, \omega) = [i\omega - \epsilon_k - \Sigma_s(\mathbf{k}, \omega)]^{-1}$. Since bosons condense, the physical electron Green's function can be simply obtained by $G(\mathbf{k}, \omega) = \delta G_f(\mathbf{q}, \omega)$, i.e., only the dynamics of spins is considered. Following previous prescriptions, one then obtains the surface Green's functions and thus the various conductance. The truncation to the lowest order cannot really be justified rigorously so far. Its merit rests mainly upon its simplicity and its usefulness in previous applications to problems related to spin fluctuations[10]. These studies indicate that it has captured the main

features of ARPES data along [100] direction and for other directions it also reproduces the observed $\cos(6\theta)$ deviation from the pure d -wave[10]. Here we shall examine its validity against tunneling data. Note also that we had neglected the spatial dependence of the pair potential, which is generally considered not important in [100] and [001] directions.

We first analyze small λ limit. Fig. 2 shows the total conductance with RPA correction for various dopings. The positions of the peak and hump are seen to scale weakly with doping. When doping increases, the height of peak increases with doping, in consistent with experiments[13], at the same time, the width of the peak increases and tends into the hump region so that the hump is smeared out in slightly overdoped region. Another feature which can also be observed in the data is that the dip/hump feature at positive bias is always weaker. The precise reason behind them can be traced back to the underlying structure of ϵ_k . In fact, detailed analysis[12] shows that the band edge extends to higher positive bias so that the dip/hump is smeared, while the band edge for negative bias essentially stays at small bias, leaving the dip/hump unsmeared.

We now numerically identify the optimum matching condition so that the zero bias Andreev conductance peak can be manifested best. For each k_y , we compute the optimal value t_{opt} such that the Andreev conductance at $V = 0$ reaches maximum. The resulting $t_{opt}(k_y)$ can be approximated by

$$t_{opt}(k_y) = a_0 + a_1 \cos(k_y) + a_2 \cos(2k_y) \quad (2)$$

This implies that including next nearest neighbor hopping along the junction is necessary. However, the forward hopping a_0 still dominates (for instance, when $\delta = 0.12$, we obtain $a_0 = 2.41$, $a_1 = -0.44$, and $a_2 = 0.34$). In Fig.3, we show the optimal manifestation of the Andreev peak for different doping. The metal side is modeled by a simple tight-binding model on the square lattice. We see that the dip/hump structure coexists with the Andreev peak. Fig. 4 shows a similar plot but now the density of state of the metal side is a constant. In this case, the Andreev peak never out wins the quasi-particle peaks resulted from $G_1(V)$ so that a plateau is observed. In both cases, the trend of the dip/hump structure with doping is consistent with what is found in Fig.2. All these qualitative features should be experimentally verified in the future as a test of the mechanism of the spin fluctuations.

To further test this particular RPA approach, we compute the c-axis tunneling spectrum. Fig. 5 shows our numerical results, in comparison to the recent STM curve by Pan *et. al.* [14]. It is quite encouraging that two curves are very similar in the shape. In particular, the step around 45 mV is reproduced in the RPA approach at slightly larger bias. This step results from the band edge, which, as we mentioned, essentially stays at small bias as one changes doping.

To summarize, we have analyzed the effects of spin fluctuations on the SN junction using the Keldysh formulation and a modified random phase approximation. The peak/dip/hump structure is reproduced and we show that it disappears gradually as one goes to slightly overdoped region. Using the same formulation, we predict that the dip/hump structure can coexist with the zero bias Andreev peak in optimal matching conditions. Our analysis on the c-axis tunneling shows good qualitative agreement between this approach and the recently observed STM tunneling curve.

It is our pleasure to thank Profs. N. C. Yeh, C.R. Hu and T. K. Lee for useful discussions. DC also wish to thank SLAC Theory Group for hospitality. This research was supported by NSC of Taiwan.

References

- [1] See recent review M. Randeria and J.C.Campuzano cond-mat 9709107.
- [2] G. E. Blonder, M. Tinkham, and T. M. Klapwijk, Phys. Rev. B **25**, 4515 (1982).

- [3] See for example, Y. Tanaka and S. Kashiwaya, Phys. Rev. Lett. **74**, 3451 (1995).
- [4] D. S. Dessau, *et al.*, Phys. Rev. Lett. **66**, 2160 (1991).
- [5] M. Randeria, *et al.*, Phys. Rev. Lett. **74**, 4951 (1995).
- [6] See for example, Y. DeWilde, *et al.*, Phys. Rev. Lett. **80**, 153 (1998).
- [7] Z. -X. Shen and J. R. Schrieffer, Phys. Rev. Lett. **78**, 1771 (1997); M. R. Norman and H. Ding, Phys.Rev.B **57**, R11089, 1998.
- [8] See for example, J. Rossat-Mignod *et al.*, Physica C **185-189**, 86 (1991).
- [9] A. Abanov and A. V. Chubukov, Phys. Rev. Lett. **83**, 1652 (1999).
- [10] J. Brinckman and P. A. Lee, Phys. Rev. Lett. **82**,2915, (1999); J. X. Li, C. -Y. Mou, and T. K. Lee, Phys. Rev. B **62**, 640 (2000).
- [11] H. Ding et al. cond-mat 0006143.
- [12] It will be shown in a separate publication that when appropriately modifying the the relation of the surface Green's functions to the bulk Green's functions, the current formalism is also applicable to the [110] direction, where the ZBCP is observed (see Ref. [3]; C. R. Hu, Phys. Rev. Lett. **72**, 1526 (1994); S. Kashiwaya, Rep. Prog. Phys. **63**, 1641 (2000) and references therein.)
- [13] N. Miyakawa et al. Phys. Rev. Lett. **83**, 1018 (1999).
- [14] S. H. Pan et al. cond-mat/0005484.
- [15] L. V. Keldysh, Sov. Phys. JETP **20**, 1018 (1965).
- [16] J. C. Cuevas, A. Martin-Rodero, and A. L. Yeyati, Phys. Rev. B **54**, 7366 (1996).
- [17] X. Z. Yan, H. Zhao, and C. R. Hu, cond-mat/0001170.
- [18] For tunneling along [100] direction, the density of state has to include an extra $\sin^2(k_x a)$ factor due to the boundary condition at $x = a$. This is different from the c-axis STM measurement, where the usual density of state without $\sin^2(k_x a)$ factor is measured.
- [19] Early RPA work can be found in H. Tanamoto et al. J. Phys. Soc. Jpn. **61**, 1886, (1992); *ibid* **62**, 717, (1993); *ibid* **62**, 1455, (1993). Our parameters are different from those used in these references, however, they yield similar Fermi surfaces in the mean field level and therefore similar qualitative consequences.

1 FIGURE CAPTIONS

Fig.1 Feynman diagrams for (a) the spin susceptibility and (b) and (c) the lowest order contributions to the self-energy from spin fluctuations.

Fig.2 The total conductance with RPA correction in the tunneling limit. Here the metal is modelled by a constant density of state with $\lambda = 0.05$.

Fig.3 The optimal manifestation of the Andreev peak with a square lattice ($t_L = 1.0$) for the metal side.

Fig.4 The optimal manifestation of the Andreev peak with constant density of state ($t_L = 1.0$) for the metal side.

Fig.5 The density of state for c-axis tunneling for $\delta = 0.12$. Inset: The STM tunneling curve observed by Pan et al[14].

$$\text{Diagram with } \chi \text{ in a circle} = \text{circle} + \text{circle} + \dots + \dots \quad (\text{a})$$

$$\Sigma_S(\mathbf{q}, \omega) = \text{Diagram with } \chi \text{ in a circle and a line with an arrow} \quad (\text{b})$$

$$\Sigma_W(\mathbf{q}, \omega) = \text{Diagram with } \chi \text{ in a circle and a line with two arrows} \quad (\text{c})$$

Fig.1

Fig. 2

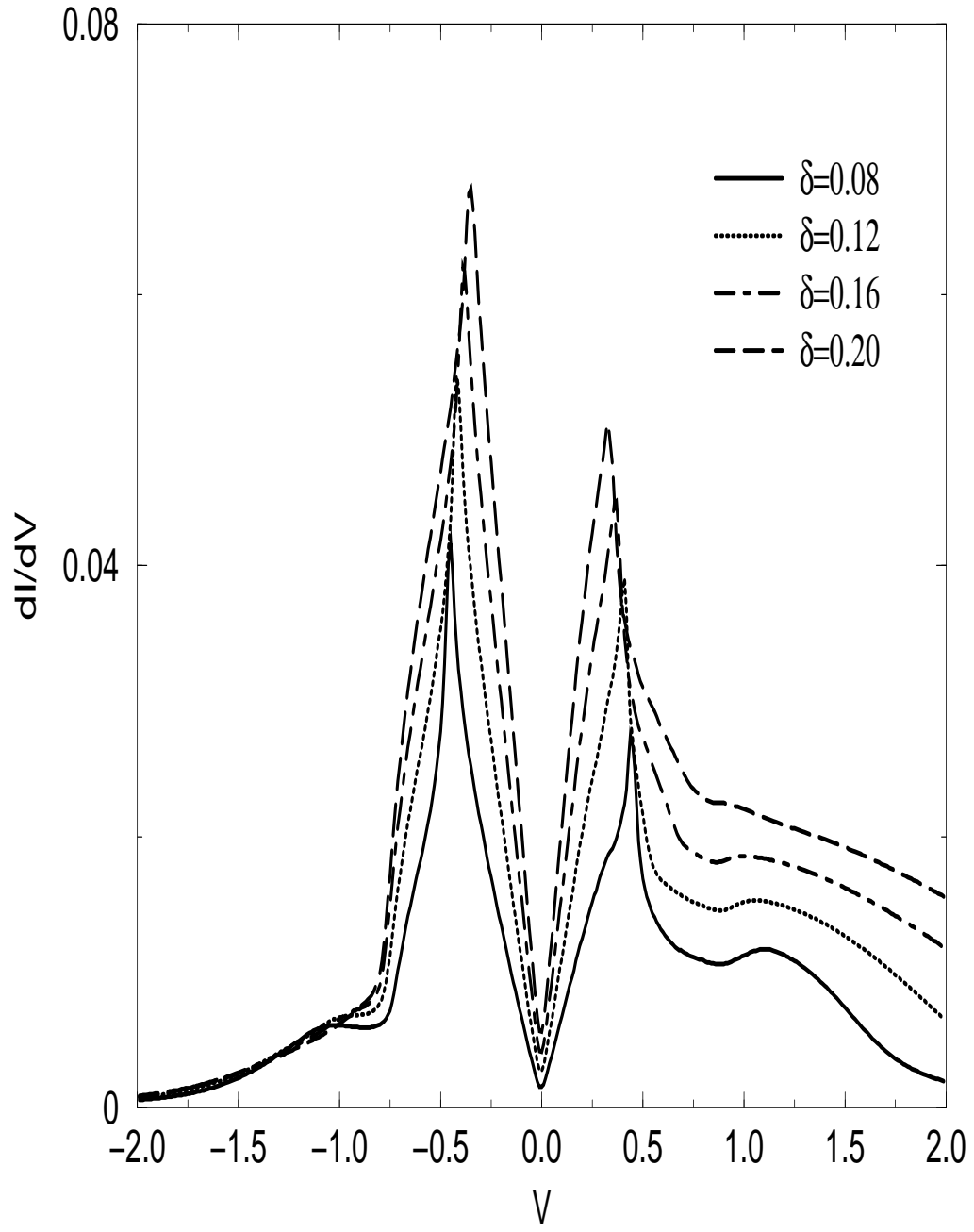


Fig. 3

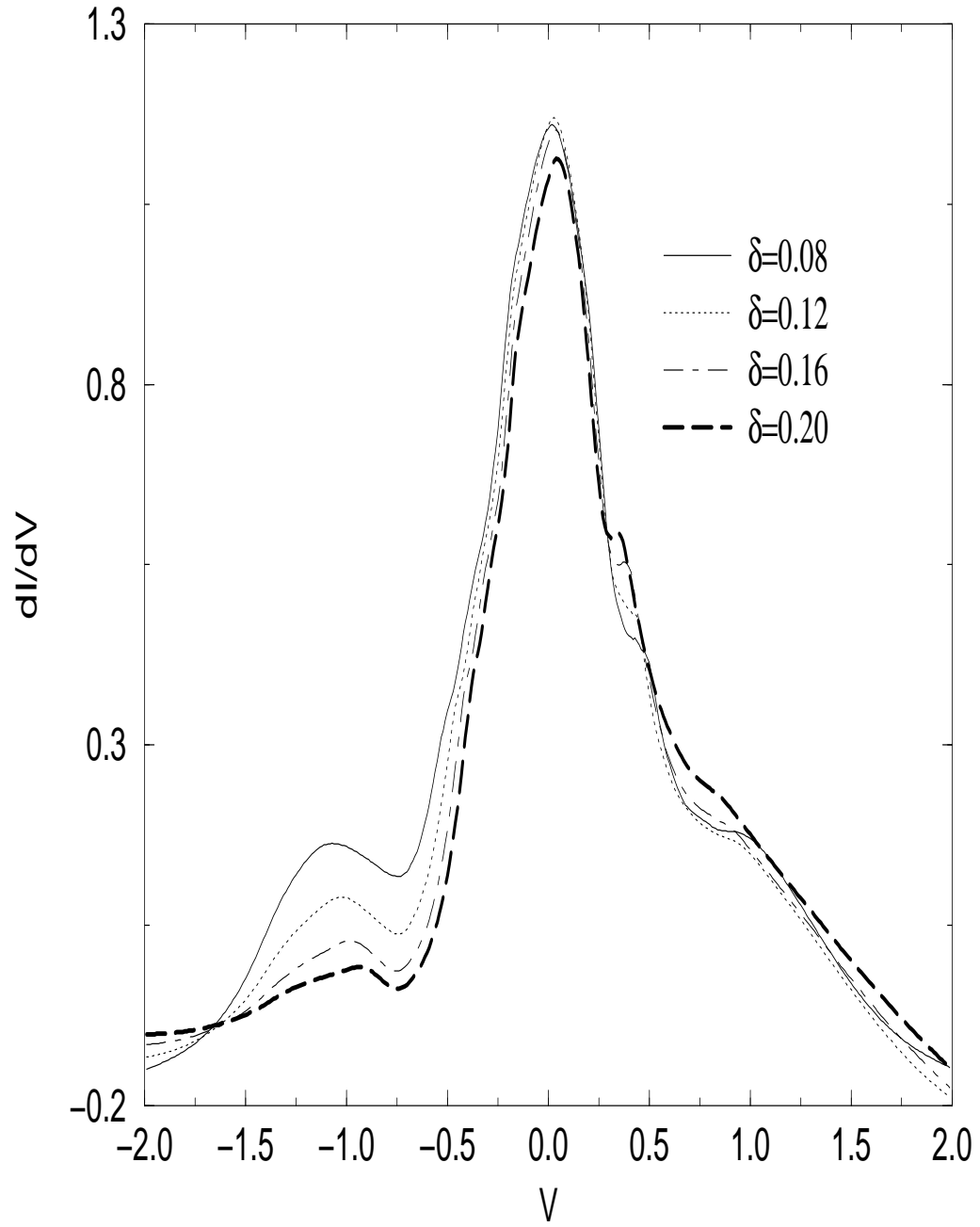


Fig. 4

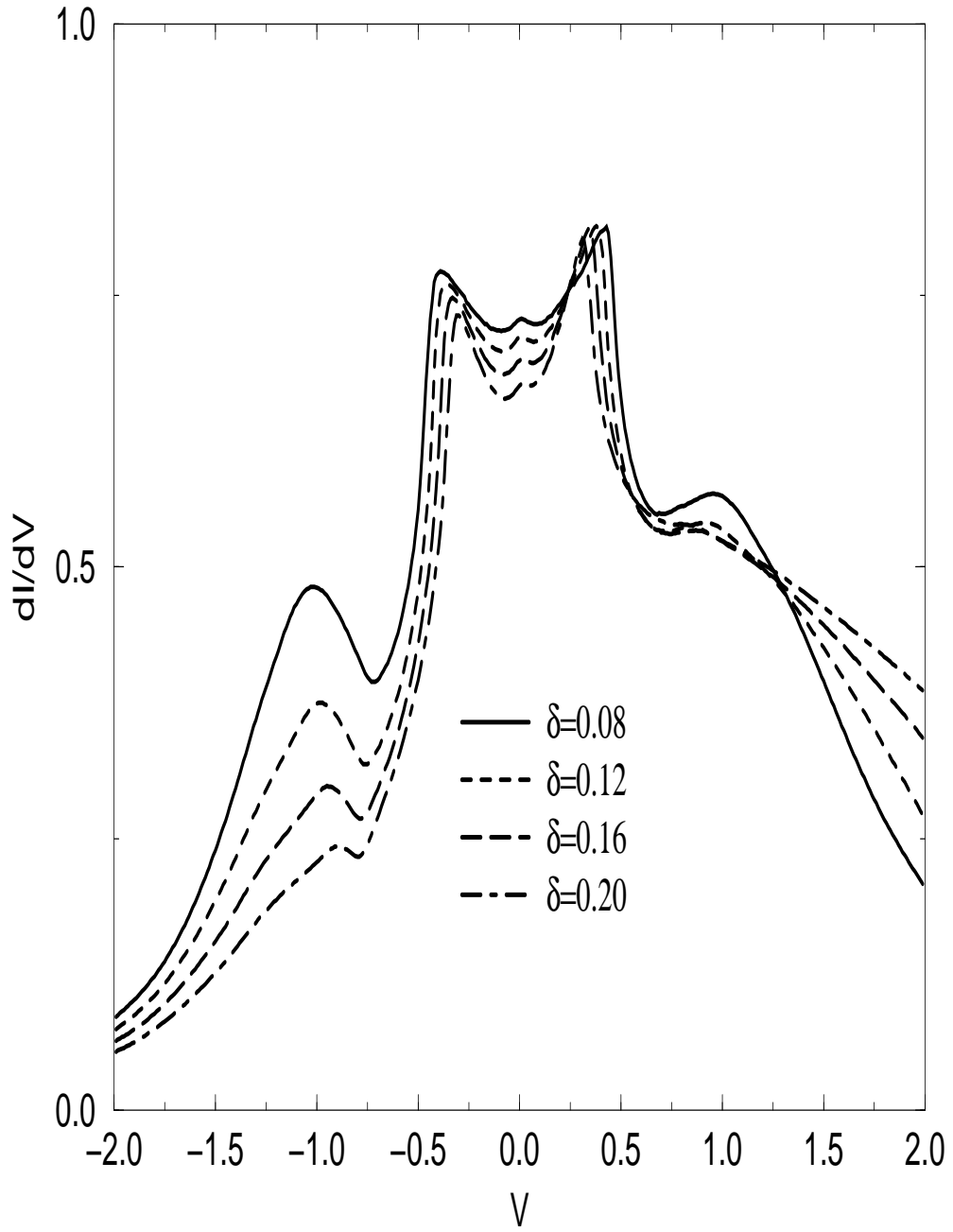


Fig. 5

